LLNL-CONF-471564

Event-by-Event Fission with FREYA

J. Randrup, R. Vogt

February 25, 2011

Scientific Workshop on Nuclear Fission dynamics and the Emission of Prompt Neutrons and Gamma Rays
Sinaia, Romania
September 27, 2010 through September 29, 2010

Disclaimer

Event-by-Event Fission with FREYA

J. Randrup [1] *and R. Vogt* [2,3]

1) Lawrence Berkeley National Laboratory, Berkeley, California 94720, USA
2) Lawrence Livermore National Laboratory, Livermore, California 94551, USA
3) University of California at Davis, Davis, CA 95616, USA

Abstract: The recently developed code *FREYA* (Fission Reaction Event Yield Algorithm) generates large samples of complete fission events, consisting of two receding product nuclei as well as a number of neutrons and photons, all with complete kinematic information. Thus it is possible to calculate arbitrary correlation observables whose behavior may provide unique insight into the fission process. The presentation first discusses the present status of *FREYA*, which has now been extended up to energies where pre-equilibrium emission becomes significant and one or more neutrons may be emitted prior to fission. Concentrating on ^{239}Pu(n,f), we discuss the neutron multiplicity correlations, the dependence of the neutron energy spectrum on the neutron multiplicity, and the relationship between the fragment kinetic energy and the number of neutrons and their energies. We also briefly suggest novel fission observables that could be measured with modern detectors.

Introduction

Nuclear fission presents an interesting and challenging physics problem which is still, about seventy years after its discovery, relatively poorly understood. Although much of the key physics involved is understood qualitatively, a quantitative description is still not in sight, despite vigorous efforts by many researchers. Because of its inherent complexity, fission provides an important testing ground for both static and dynamical nuclear theories. Furthermore, fission is also important to society at large because of its many practical applications, including energy production and counter proliferation, topics of current urgency.

Whereas the more traditional treatments of fission have sought to describe only fairly integral fission properties (see in particular Ref. [1]), such as the average energy release and the average differential neutron yield, many modern applications require more exclusive quantities, such as fluctuations in certain observables (e.g. neutron multiplicity) and correlations between different observables (e.g. neutrons and photons). There is thus a need for developing models that include the treatment of fluctuations and correlations.

Simulation models offer a powerful means for meeting this challenge because they generate large samples of complete fission events and subsequent event-by-event analysis can then provide any specific correlation observable of interest. Furthermore, due to the more detailed quantities that can be addresses, such models may provide valuable guidance with regard to which observables are most crucial for further progress in the understanding of fission.

We have developed a calculational framework within which large samples of complete fission events can be generated, starting from a fissionable nucleus at a specified excitation energy [2]. The associated computer code is named *FREYA* (Fission Reaction Event Yield Algorithm). We present here the model in a fairly basic form which, though quite simplistic in many regards, is already capable of producing interesting results. *FREYA* was employed in a recent study of sequential neutron emission following neutron-induced fission of ^{240}Pu [3] and it has recently been extended to pre-fission neutron emission [4].

We give here a brief overview of *FREYA*; more complete discussions may be found in the published literature [2–4]. Since the model is under active development, the results shown here are illustrative only.

Model components

The main components of *FREYA* are described below. The discussion follows the successive temporal stages of the fission process, from the agitation by the incident neutron to the deexcitation of the fission fragments.

Pre-fission emission

When the initial compound nucleus (^{240}Pu* here) is sufficiently excited, it may emit one or more neutrons before fission occurs. We take this into account in a manner similar to the post-fission evaporation (see later). At sufficiently high excitations we include pre-equilibrium emission [4]. At each stage, neutron emission competes with fission according to a simple model for the energy-dependent branching ratio [5]. Figure 1 (left) shows the resulting multi-chance fission probabilities compared to the *GNASH* calculations used in the ENDF-B/VII.0 evaluation [6]. The two calculations give rather similar probabilities. The kinematics, including the recoil momentum of the nucleus, is treated in an exact manner, while angular-momentum effects are ignored.

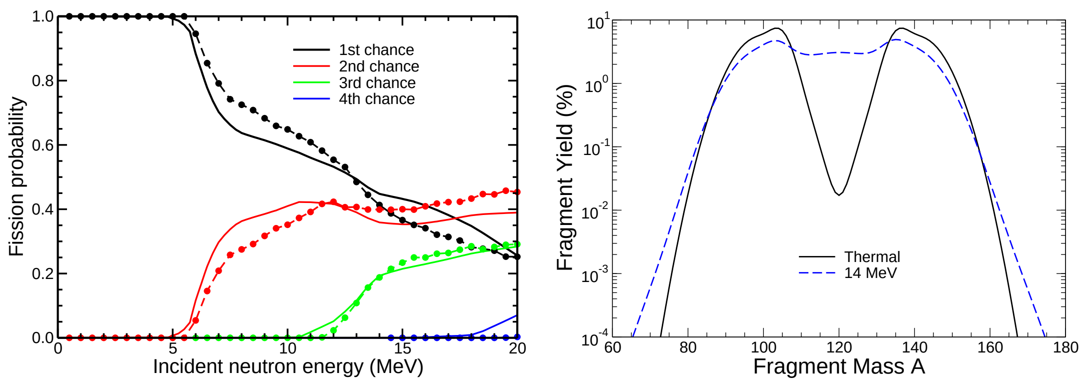

Figure 1: *Left: Probabilities for $N^{\rm th}$-chance fission as functions of incident neutron energy $E_{\rm n}$; the solid curves are GNASH calculations used in the ENDF-B/VII.0 evaluation while the dashed curves with circles are FREYA calculations. Right: Calculated fragment mass yields caused by thermal and 14 MeV neutrons (the latter includes contributions from multi-chance fission).*

Mass and charge partition

At the present stage of development, the fragment mass distribution $P(A_{\rm f})$ is based on experimentally observed yields. We employ a five-gaussian fit to $P(A_{\rm f})$ [7,8], using energy dependent coefficients so the distribution evolves from being asymmetric to predominantly symmetric as the energy is raised, as illustrated in Fig. 1 (right). Once the fragment masses, $A_{\rm L}$ and $A_{\rm H}$ have been sampled from $P(A_{\rm f})$, the fragment charges are sampled from a (truncated) normal distribution having a dispersion of $\sigma_Z = 0.50$ [9]. The Q-value associated with that particular split can then be calculated, $Q_{\rm LH} = M(^{240}{\rm Pu}^*) - M_{\rm L} - M_{\rm H}$. We use experimental data for the fragment masses where available [10] and supplement with calculated values [11] as needed.

Fragment kinetic energy

The Q-value is divided between the relative fragment kinetic energy *TKE* and internal fragment excitation. Since we do not yet have a sufficiently quantitative model for this division, we seek to match *TKE* to the experimental data [12–14]. A small overall energy-dependent adjustment *dTKE* is made subsequently in order to reproduce the measured average total neutron multiplicity $\bar\nu$ (see below), $TKE(A) \to TKE(A) + dTKE(E_{\rm n})$, where $dTKE \approx 1$–2 MeV. Figure 2 shows the resulting mass dependence of the total fragment kinetic energy. The two fragments are assumed to emerge isotropically back-to-back in the reference frame of the fissioning nucleus and to have been fully accelerated before neutron evaporation commences.

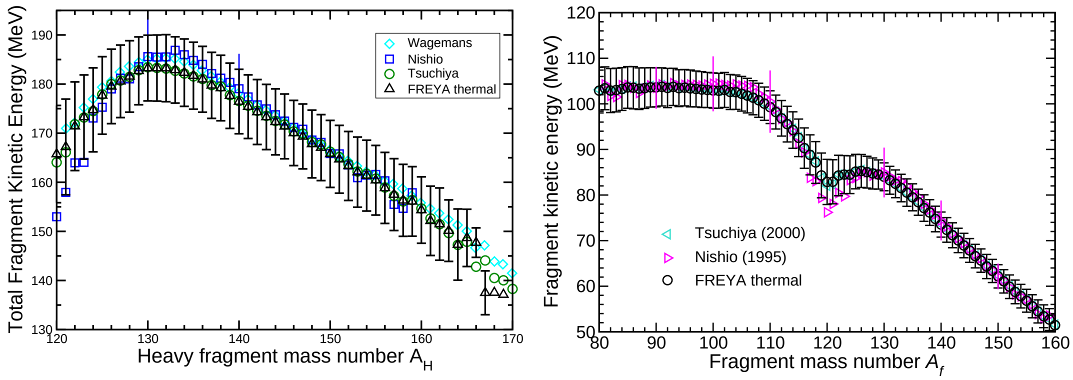

Figure 2: *The measured average TKE as a function of the heavy fragment mass number [12–14] compared to FREYA calculations at thermal energies, shown with the calculated dispersion in TKE for each A_{H} (left). The average fragment kinetic energy as a function of the fragment mass A_{f} from Refs. [13, 14] as well as FREYA results, at thermal energies (right).*

Energy partition

We assume that the remaining energy appears as statistical excitation of the two fragments. We first divide this energy between the two fragments in proportion to their respective heat capacities which are proportional to the Fermi-gas level-density parameters a_A for which we use the values calculated in Ref. [15], $\overline{Q}_{\mathrm{L}}:\overline{Q}_{\mathrm{H}} = a_{\mathrm{L}}:a_{\mathrm{H}}$. We then adjust the partioning in favor of the light fragment which tends to become hotter than the heavy one, $\overline{Q}_{\mathrm{L}} \to x\overline{Q}_{\mathrm{L}}$ (with a balancing decrease of Q_{H}), where the the global parameter x exceeds unity by 10–20%.

Subsequently we add statistical fluctuations to these mean excitations, assuming that they are given by the associated thermal variances, $\sigma_i^2 = 2\overline{Q}_i T_{\mathrm{LH}}$. The fluctuations δQ_i are therefore sampled from normal distributions with variances σ_i^2. The fragment excitations in a given event are then $Q_i = \overline{Q}_i + \delta Q_i$. Energy conservation implies that the distribution of the total kinetic energy K_{LH} is a gaussian (such a form was already assumed in Ref. [16]) with the variance $\sigma_{\mathrm{K}}^2 = \sigma_{\mathrm{L}}^2 + \sigma_{\mathrm{H}}^2$. The resulting fragment excitations are shown in Fig. 3 (left).

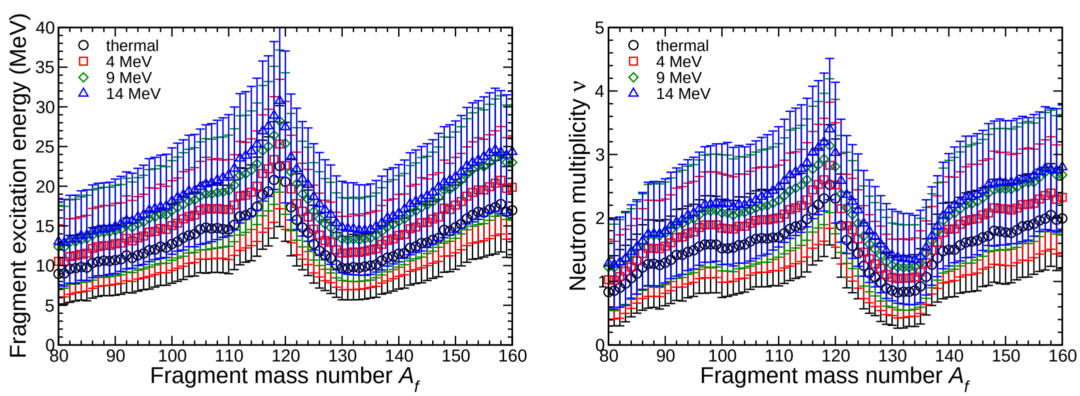

Figure 3: *The pre-evaporation excitation energy of a fully accelerated fission fragment (left) and the total multiplicity of (both pre- and post-fission) neutrons (right), calculated with FREYA for various incident neutron energies E_{n}. Both are shown as functions of the fragment mass number A_{f}. The vertical bars indicate the dispersions of the respective distributions.*

Neutron evaporation

We assume that the two excited fragments do not begin to de-excite until after they have been fully accelerated by their mutual Coulomb repulsion and their shapes have reverted to their equilibrium form. Furthermore, we ignore the possibility of charged-particle emission from the fission fragments. Each of the fully relaxed and accelerated fission fragments typically emits one or more neutrons as well as a (larger) number of photons. We assume that neutron evaporation has been completed before photon emission sets in, thus obviating the need for knowing the ratio of the decay widths, $\Gamma_\gamma/\Gamma_{\rm n}$.

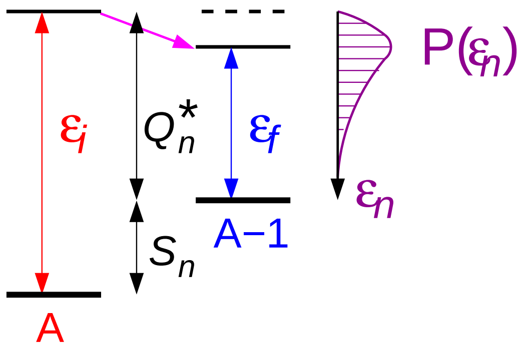

$$Q_{\rm n}^* \;=\; \varepsilon_i^* - S_{\rm n} \;=\; \varepsilon_f + \epsilon_{\rm n}$$

$$T_f^{\rm max} \;=\; \sqrt{Q_{\rm n}^*/a_A}$$

$$dP(\epsilon_{\rm n})/d\epsilon_{\rm n} \;\sim\; \epsilon_{\rm n}\,{\rm e}^{-\epsilon_{\rm n}/T_f^{\rm max}}$$

$$\epsilon_{\rm n} \;=\; -T_f^{\rm max}\ln(\eta_1\eta_2)\;,\quad \eta_i\in(0,1]$$

Figure 4: *The energetics relevant to the evaporation of a neutron from a nucleus with mass number A and excitation ε_i. The resulting neutron kinetic energy $\epsilon_{\rm n}$ peaks at twice the maximum temperature in the daughter nucleus and can be quickly sampled from the associated spectral distribution $P(\epsilon_{\rm n})$ by means of standard uniform random numbers η.*

For each fission fragment, neutron radiation is treated by iterating a simple treatment of a single neutron evaporation until no further neutron emission is energetically possible, as illustrated in Fig. 4. Once the Q-value is known, it is straightforward to sample the momentum of an evaporated neutron, assuming that it is isotropic in the frame of the emitting nucleus and assuming that the kinetic energy has the distribution $P(\epsilon_{\rm n}) \sim \epsilon_{\rm n}\exp(-\epsilon_{\rm n}/T)$. Relativistic kinematics ensures exact conservation of energy and momentum. The resulting neutron multiplicity ν, shown in Fig. 3 (right), has a mass dependence similar to that of the fragment excitation energy.

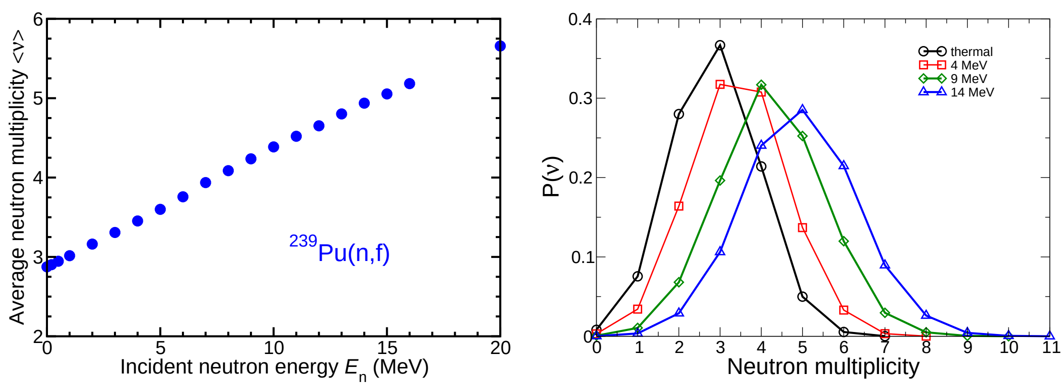

Figure 5: *The average neutron multiplicity as a function of the incident neutron energy $E_{\rm n}$ (left) and the neutron multiplicity distribution P(ν) for selected values of $E_{\rm n}$ (right).*

Above $E_\mathrm{n} \approx 0.2$ MeV the expected neutron multiplicity grows steadily with the kinetic energy of the incident neutron, from nearly three for thermal neutrons to almost six for 20 MeV, as shown in Fig. 5 (left). The entire multiplicity distribution $P(\nu)$ is shown in the right panel for several selected energies. An examination of $P(\nu)$ shows that it is significantly narrower than the corresponding Poisson distribution. This is presumably because the reduction in excitation energy caused by an emission is dominated by the separation energy $S_\mathrm{n} \approx 6.5$ MeV, which is significantly larger than the average of the statistical part of the energy reduction, $2T \approx 2$ MeV.

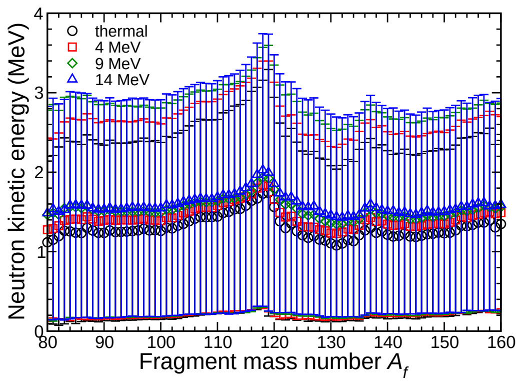

E_n (MeV):	0.5	14	14
ν	1st	1st	Nth
1	2.22	2.49	2.62
2	2.21	2.58	2.60
3	2.14	2.58	2.52
4	2.07	2.56	2.45
5	1.99	2.52	2.38
6	1.90	2.49	2.32
7	1.83	2.47	2.28
8		2.44	2.27
all	2.11	2.52	2.37

Figure 6: *The dependence of the neutron kinetic energy on the fragment mass number for various incident energies, with the bars indicating the respective energy dispersions (left) and the mean neutron kinetic energy for various total neutron multiplicities ν for $E_\mathrm{n} = 0.5$ MeV and $E_\mathrm{n} = 14$ MeV including either only 1st-chance fission or unlimited pre-fission emission (right).*

Generally, the first neutron evaporated from a fragment will tend to have a higher energy than the second one, and so on, see Fig. 6 (right). For this reason and due to the fluctuation in mass partition the resulting overall neutron spectral shape will not be of a simple form but have many components. While this complexity is automatically accounted for in event-by-event simulations, the feature cannot be obtained in treatments that consider only averages (e.g. [1]).

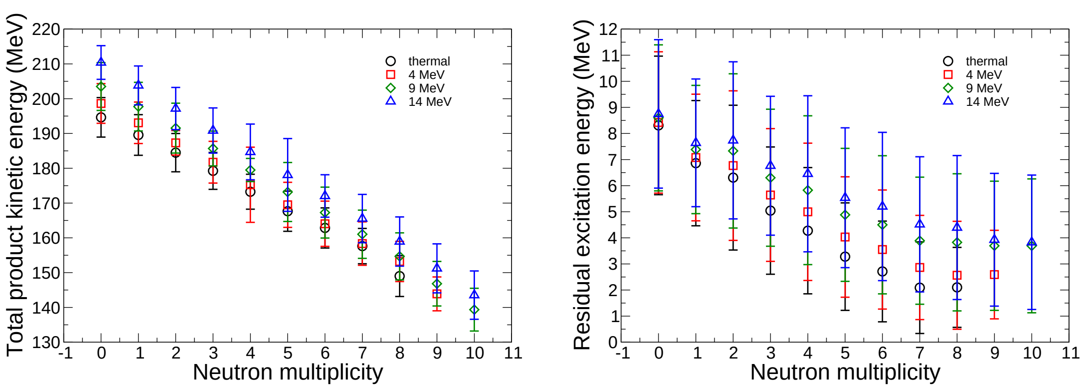

Figure 7: *The neutron-multiplicity dependence of the total kinetic energy of the two fission products (left) and their combined excitation after the neutron evaporation cascade (right), as obtained with FREYA for various incident neutron energies. The bars show the dispersions.*

Events having lower-than-average fragment kinetic energies will, by energy conservation, tend to have higher-than-average initial fragment excitations and, therefore, they will on average produce more neutrons. This expected anti-correlation between the neutron multiplicity and the product kinetic energy is indeed brought out by the *FREYA* results, as illustrated in Fig. 7 (left).

Photon emission

When the neutron evaporation cascades have been completed, the product nuclei are left with some residual excitation which will give rise to subsequent photon radiation. As illustrated in Fig. 7 (right), the degree of residual excitation tends to decrease with the multiplicity of emitted neutrons, as one might have expected on the basis of energy conservation. Consequently, one should also expect that the number of photons emitted will be anti-correlated with the neutron multiplicity.

At the present stage of development, *FREYA* treats the photon emission process only in a very rudimentary manner, considering it as if it were simply evaporation of massless particles. While this approach would certainly not be adequate for calculating the emission rates, it may provide a reasonable approximation for the spectral *shape* which should be primarily governed by phase space. Furthermore, as an elementary analysis will reveal, the ultra-relativistic limit appropriate for massless particles is as easy to simulate as the non-relativistic limit employed for the neutrons, the key feature being $\epsilon_\gamma \sim \ln(\eta_1\eta_2\eta_3)$. Therefore, in this approximate manner, *FREYA* can also treat the photon emission cascades in a numerically very efficient manner.

Observables

FREYA produces a sample of complete fission events, each one being described by the four-vectors of the two product nuclei and of all the individual neutrons and photons emitted in that event. Special effort has been made to make the numerical code fast and, as a result, one million events can be generated within about ten seconds on a standard laptop computer. While such statistics suffice for calculating most quantities of interest, it should be possible to devise more efficient calculational strategies for the generation of specific classes of rare events that might be of special interest.

Because *FREYA* produces complete events, it is straightforward to extract any observable of interest. The above exposition has presented a variety of observables. The special advantage of an event-by-event treatment is that it readily permits the extraction of fluctuations in any observable and the correlations between different observables, quantities that are not accessible in models designed to merely provide the mean behavior. Furthermore, because the elementary physical processes are treated explicitly, *FREYA* also tends to yield improved results for certain average quantities, such as the neutron energy spectrum.

As an example of a readily obtainable correlation observable, we consider here the angular correlation $C(\phi_{12})$ between two emitted neutrons. Fig. 8 shows the result for ^{239}Pu(n$_{\rm th}$,f). The correlation functions shown in the left panel include *all* the neutrons emitted in each event with kinetic energies above specified thresholds of 0.5, 1.0 and 1.5 MeV. The extracted $C(\phi_{12})$ is remarkably insensitive to the total neutron multiplicity ν (though it is somewhat stronger for events having very low multiplicity) and the correlations grow slightlystronger as the threshold energy is raised. Its form can readily be understood by considering events that have only two neutrons (with energies above 1 MeV), as shown in Fig. 8 (right): When both neutrons are emitted by the same fragment they exhibit a close angular correlation. It is strongest when the common source is the light fragment, presumably because of its higher speed. Conversely, when the two neutrons come from different fragments they exhibit a strong directional anti-correlation that is enhanced by the relative fragment motion. The combined correlation function for $\nu=2$, $C_{\nu=2}(\phi_{12})$ is shown in both panels for reference.

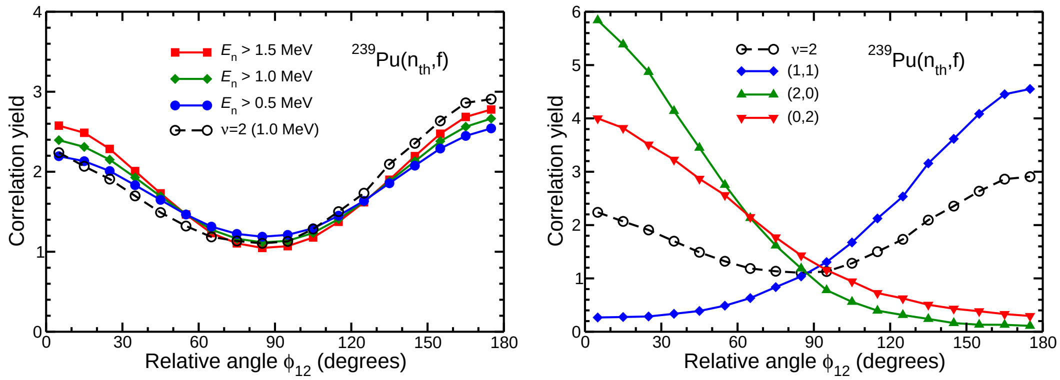

Figure 8: *Neutron angular correlations. Left: The correlation yield C(ϕ_{12}) for neutrons having energies above a specified threshold. Right: C(ϕ_{12}) for events that have a total multiplicity of two (each one with energy above one MeV),* $\nu \equiv \nu_\mathrm{L} + \nu_\mathrm{H} = 2$ *(solid black dots), together with the correlation for events where the two neutrons come from different fragments,* $(\nu_\mathrm{L}, \nu_\mathrm{H}) = (1,1)$ *(blue diamonds) and for events where both neutrons come from the same fragment, either the light,* $(\nu_\mathrm{L}, \nu_\mathrm{H}) = (2,0)$ *(green) or the heavy,* $(\nu_\mathrm{L}, \nu_\mathrm{H}) = (0,2)$ *(red).*

A second example is the correlation between the neutron and photon multiplicities. As already mentioned above, a larger-than-average neutron multiplicity tends to yield a lower-than-average product excitation and, therefore, one would expect the neutron and photon multiplicities to be anti-correlated. This is indeed borne out by the *FREYA* calculations. Contrary to the mean neutron multiplicity $\bar{\nu}$, which increases steadily with the incident neutron energy E_n, the calculated average photon multiplicity is fairly independent of E_n. The magnitude of the calculated multiplicity correlation coefficient (which is thus negative) decreases steadily with E_n. A quantitative discussion requires a more refined treatment of the photon emission.

Outlook

Over the past few years, experimental capabilities have improved dramatically while the practical applications of fission have broadened significantly. As a consequence, there has been an growing need for calculations of increasingly complex observables that are beyond the scope of the traditional fission models.

To meet this need, we have developed a new calculational framework, *FREYA*, which can generate large samples of individual fission events. From those it is then possible to extract any specific observable of interest, in particular correlation observables of any complexity, without the need for further approximation. In developing *FREYA*, we have sought to make the numerics sufficiently fast to facilitate use of the code as a practical calculational tool.

Although the current version of *FREYA* is still only preliminary, it has already proven to be quantitatively useful. For example, the combination of the Monte Carlo fission model with a statistical likelihood analysis presents a powerful tool for the evaluation of fission neutron data which was used to develop an estimate of the fission neutron spectrum with uncertainties several times smaller than current experimental uncertainties [3]. *FREYA* has already proven to be capable of making interesting predictions for correlations in variety of contexts and we foresee an increased number of applications.

Acknowledgments

We acknowledge many helpful discussions with D.A. Brown, M.-A. Descalle, D. Gogny, E. Ormand, P. Möller, E.B. Norman, J. Pruet, W.J. Swiatecki, P. Talou and W. Younes. This work was performed under the auspices of the US Department of Energy by the Lawrence Livermore National Laboratory under Contract DE-AC52-07NA27344 (R.V.) and by the Lawrence Berkeley National Laboratory under Contract DE-AC02-05CH11231 (J.R.) and was also supported in part by the National Science Foundation Grant NSF PHY-0555660 (R.V.).

References

[1] D.G. Madland and J.R. Nix, Nucl. Sci. Eng. **81** (1982) 213.

[2] J. Randrup and R. Vogt, Phys. Rev. C **80** (2009) 024601.

[3] R. Vogt, J. Randrup, J. Pruet and W. Younes, Phys. Rev. C **80** (2009) 044611.

[4] R. Vogt, J. Randrup, D.A. Brown and E. Ormand, in preparation (2010).

[5] W.J. Swiatecki, K. Siwek-Wilczynska and J. Wilczynski, Phys. Rev. C **78** (2008) 054604.

[6] M.B. Chadwick *et al.*, Nucl. Data Sheets **107** (2006) 2931.

[7] U. Brosa *et al.*, Phys. Rep. **97** (1990) 1; U. Brosa, Phys. Rev. C **32** (1985) 1438.

[8] F.-J. Hambsch *et al.*, Nucl. Phys. A **491** (1989) 56.

[9] W. Reisdorf, J.P. Unik, H.C. Griffin and L.E. Glendenin, Nucl. Phys. A **177** (1971) 337.

[10] G. Audi and A.H. Wapstra, Nucl. Phys. A **595** (1995) 409.

[11] P. Möller, J.R. Nix, W.D. Myers and W. J. Swiatecki, At. Data Nucl. Data Tab. **59** (1995) 185.

[12] C. Wagemans *et al.*, Phys. Rev. C **30** (1984) 218.

[13] K. Nishio, Y. Nakagome, I. Kanno and I. Kimura, J. Nucl. Sci. Technol. **32** (1995) 404.

[14] C. Tsuchiya *et al.*, J. Nucl. Sci. Technol. **37** (2000) 941.

[15] T. Kawano, S. Chiba and H. Koura, J. Nucl. Sci. Technol. **43** (2006) 1.

[16] S. Lemaire *et al.*, Phys. Rev. C **72** (2005) 024601.

[17] N. Koura, M. Uno, T. Tachibana, and M. Yamada, Nucl. Phys. A **674**, 47 (2000).